ACS APPLIED MATERIALS & INTERFACES

Research Article

www.acsami.org

Fabrication of Well-Ordered Binary Colloidal Crystals with Extended Size Ratios for Broadband Reflectance

Zhongyu Cai,*[,†,‡] Yan Jun Liu,[§] Xianmao Lu,[†] and Jinghua Teng*[,§]

[†]Department of Chemical and Biomolecular Engineering, National University of Singapore, 4 Engineering Drive 4, Singapore 117576

[‡]Department of Chemistry, University of Pittsburgh, Pittsburgh, Pennsylvania 15260, United States

[§]Institute of Materials Research and Engineering, Agency for Science, Technology and Research (A*STAR), 3 Research Link, Singapore 117602

Supporting Information

ABSTRACT: Binary colloidal crystals (BCCs) possess great potentials in tuning material properties by controlling the size ratio of small to large colloidal spheres ($\gamma_{S/L}$). In this paper, we present a method for the fabrication of BCCs with much more extended size ratios than those obtained in conventional convective self-assembly method. It is found that $\gamma_{S/L}$ can be extended to 0.376 by adding TEOS sol into the colloidal suspension. The resulting polystyrene/silica (PS/SiO_2) BCCs show distinctive reflections, indicating their well-ordered structure. The extended size ratios render more flexibility in engineering the photonic bandgap structures of BCCs and hence provide a better platform for developing a range of applications such as photonics, spintronics, sensing and bioseparation.

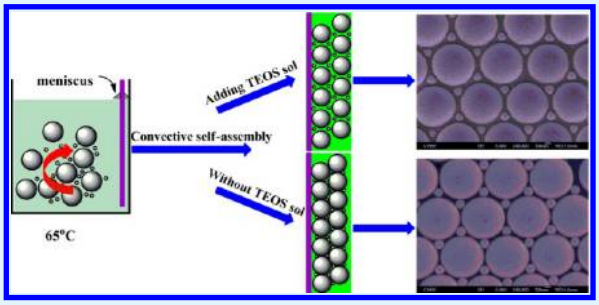

KEYWORDS: *binary colloidal crystals, improved convective self-assembly, size ratio, photonic bandgap, sensing*

1. INTRODUCTION

Binary colloidal crystals (BCCs) have attracted considerable interest in recent years.[1−18] BCCs can be fabricated by coassembling large (L) and small (S) particles made of the same or different materials. Compared to colloidal crystals (CCs) assembled from particles with a single size, BCCs offer higher flexibility in engineering the photonic bandgap structures.[4,8,9,19] Therefore, distinct optical properties can be demonstrated in BCCs. They have found wide applications in sensing, protein patterning, and bioseparation.[20−22] Unfortunately, previous studies have shown that well-ordered BCCs can be achieved only from small and large particles with sizes below a certain ratio.[9,10,22] According to both theoretical and experimental results obtained from horizontal codeposition method, Wang L. et al. have found that the size ratio ($\gamma_{S/L}$) between small spheres to large spheres should be between 0.154 and 0.225 in order to form a well-ordered BCC structure.[9] Accelerated evaporation approach may yield a rich variety of BCCs, but it is unaffordable to produce BCCs with $\gamma_{S/L}$ above 0.30.[10] Wang J. et al. investigated the effect of $\gamma_{S/L}$ on the morphology of BCCs formed with a vertical lifting technique.[22] They first simulated the BCC crystalline structure and found the theoretical lower and upper limits were $0.1547 < \gamma_{S/L} < 0.4142$. However, the experimental results demonstrated that this approach requires certain size ratio as well since ordered BCCs can only be fabricated with $0.1547 < \gamma_{S/L} < 0.223$ using this vertical lifting method.

Layer-by-layer (LbL) approach, where a monolayer of large spheres was first prepared and then another layer of small spheres was placed on top, seems to be a promising approach to fabricate BCCs in large area, theoretically, at any size ratio.[12,14,23−28] However, the control of the crystalline quality of BCCs fabricated based on LbL is much more complicated because the next layer of BCCs is determined by the ordering of the underlying layer.[18,25,28] It is unaffordable to fabricate multilayer BCCs with good crystalline quality by using LbL approach. In addition, this method is time-consuming and laborious for the preparation of 3D BCCs.[12,23,28,29] Very recently, several self-assembly methods have been developed to fabricate high-quality nonclose packed CCs and/or their inverse opals.[8,15,29−34] In particular, an improved convective self-assembly method by adding an organometallic sol−gel to the colloidal suspension shows great promise in forming high-quality nonclose packed BCCs,[8,31,33] which may allow the fabrication of BCCs with much extended range of size ratio.

Recently, we reported an improved convective self-assembly method, and investigated the effects of the concentration of PS colloidal spheres and the amount of tetraethyl orthosilicate (TEOS) sol added during self-assembly on the fabrication of crack-free inverted BCC structures via this method.[8] During the self-assembly, the size ratio of small to large spheres was kept

Received: March 19, 2014
Accepted: June 18, 2014
Published: June 18, 2014

constant ($\gamma_{S/L} \approx 0.23$). The current work presented here is the continuation of the previous work but with the focus on the effect of the size ratio of small to large spheres and subsequent optical properties of the resulting BCCs. It revealed a very interesting and exciting phenomenon that the size ratios of small to large spheres can be greatly extended, which makes the fabrication much more robust and flexible for various applications.

In this study, we report the fabrication of BCCs with much extended size ratios using an improved convective self-assembly method. This method is similar to the reported vertical deposition method except that water-soluble TEOS sol is added into the colloidal suspension before the self-assembly process. BCCs fabricated by this method combine the merit of convective self-assembly method on high crystallinity with the extended size ratio. Our results show that the size ratio can be extended to 0.376, which is much higher than that reported ($0.155 < \gamma_{S/L} < 0.225$) in the horizontal deposition method or vertical lifting method. The tunable size ratio range ($0.155 < \gamma_{S/L} < 0.376$) is also broader than that in LbL techniques reported earlier ($0.48 < \gamma_{S/L} < 0.54$).[14] The extended size ratios give us much more flexibility to engineer the photonic bandgap structures of BCCs[19] and hence provide a better platform for developing various applications, such as bioseparation,[21] bio/chemosensing,[35] protein patterning,[36] plasmonics,[31] etc. A comparison was made between BCCs fabricated by the conventional and the improved convective self-assembly methods, and significant insights on the unique nonclose packed structural properties and optical properties (broadband reflectance) of BCCs fabricated with the improved convective self-assembly method have been revealed and analyzed. In addition, the potential mechanism of this method has been presented as well.

2. EXPERIMENTAL SECTION

2.1. Materials. All chemicals, including styrene (99%, Sigma-Aldrich), potassium persulfate (99%, Sigma-Aldrich), ethanol (99.95%, Sigma-Aldrich), 2-propanol (≥99.9%, Sigma-Aldrich), n-butanol (≥99.9%, Sigma-Aldrich), sulfuric acid (98%, Merck), hydrogen peroxide (35%, Scharlau Chemie S.A.), and TEOS (98%, Sigma-Aldrich) were used as purchased. Microscope cover glasses (22 mm × 22 mm × 0.3 mm, Deckgläser) were used as substrate for the fabrication of polystyrene (PS) BCCs. The glass substrates were treated in a piranha solution (3:1 v/v 98% H_2SO_4/35% H_2O_2) at 60 °C for 2 h before use.

2.2. Fabrication of Binary Colloidal Crystals. PS colloidal spheres were synthesized via the emulsifier-free emulsion polymerization method.[37] Briefly, 22 g of styrene and 200 mL of deionized water were added into a 500 mL flask, which was placed in a water bath at 60 °C with the protection of nitrogen gas. Then 0.14 g of potassium persulfate dissolved in 50 mL of deionized water was added into the mixture under stirring at 300 rpm. After stirring for 30 h, monodisperse PS colloidal spheres with an average diameter of 789 nm (the standard deviation was less than 2%) were obtained. By varying the amount of styrene monomer, PS colloidal spheres with different sizes (168, 178, 227, 297, 346, and 485 nm) were synthesized with the same method. BCCs were fabricated based on conventional and improved convective self-assembly methods, respectively. In a typical process, PS aqueous colloidal suspensions with two different particle sizes (large and small) were mixed together in a vial. The number ratio of small to large colloidal spheres is denoted as $N_{S/L}$. A glass substrate was then vertically suspended in the vial containing the PS colloidal suspension. The solvent was evaporated slowly over a period of 24 h at 65 °C in an oven. A thin film of PS BCCs was allowed to deposit onto the suspended substrate. For the fabrication of PS/SiO_2 BCCs, TEOS sol was prepared first by mixing TEOS, absolute ethanol, and 0.1 M HCl (1:2:1 v:v:v) with sonication for 30 min. A colloidal suspension of 789 nm PS (0.289 mL, 4.330 vol %, purified by centrifugation) was then mixed with certain amount of 168 nm PS colloidal spheres (0.024 mL, 1.010 vol %, at $N_{S/L} = 2$). The PS colloidal suspension was diluted with 10 mL deionized H_2O (the large PS colloidal sphere concentration is ~0.122 vol %). Then 0.08 mL of hydrolyzed TEOS sol (containing 0.02 mL of pure TEOS) was mixed with PS suspension and sonicated for 5 min. The deposition of BCC films followed the same procedure as that used for the fabrication of PS BCCs without adding TEOS sol.

Scheme 1. Fabrication of BCCs with Conventional and Improved Convective Self-Assembly Methods

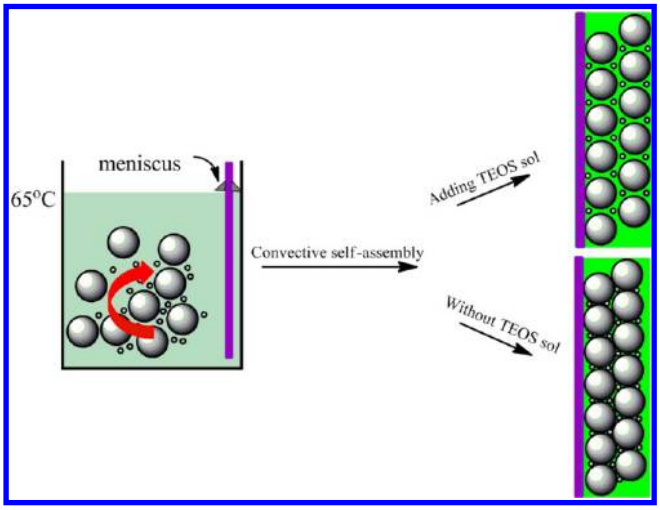

2.3. Characterization. Scanning electron microscope (SEM) images of the PS and PS/SiO_2 BCCs were recorded with a JEOL JSM-6700F field-emission SEM (FESEM). Optical spectra of the PS BCCs were obtained on a Shimadzu UV-3101 UV−vis−near-IR (UV−vis−NIR) spectrophotometer.

3. RESULTS AND DISCUSSION

3.1. PS BCCs (168/789, 227/789, and 297/789 nm) Fabricated by Conventional Convective Self-Assembly Method. Figure 1 shows the morphology of the PS BCCs prepared by conventional convective self-assembly method. At $N_{S/L} = 2$, a well-ordered 3D structure was clearly revealed from top- and side-view SEM images of PS BCCs fabricated with 168 and 789 nm colloidal spheres (Figure 1a, b). All the large colloidal spheres are closely packed to form face-centered cubic (fcc) crystalline structure, which can be confirmed from both top and cross-sectional FESEM views. Within the structure, each interstitial void of the large spheres is filled with one small sphere. At $N_{S/L} = 4$, three small spheres perfectly fit in each interstitial void with highly ordered arrangement (Figure 1c, d). The results show that close-packed BCCs can be fabricated through conventional convective self-assembly method. This is in agreement with previous studies.[8,9,13] However, only small crack-free domains (~20 × 20 μm^2) can be achieved (see Figure S1a in the Supporting Information).

For close-packed BCCs, geometrical analysis indicates that the theoretical upper limit of $\gamma_{S/L}$ is 0.225.[22] Wang and co-workers also predicted that it is impossible to obtain BCCs when the size ratio is larger than 0.225 using conventional convective self-assembly method.[9] However, no further experimental data are available to support this statement. We therefore conducted comparable experiments to investigate the BCC structures with larger size ratios. We further studied the

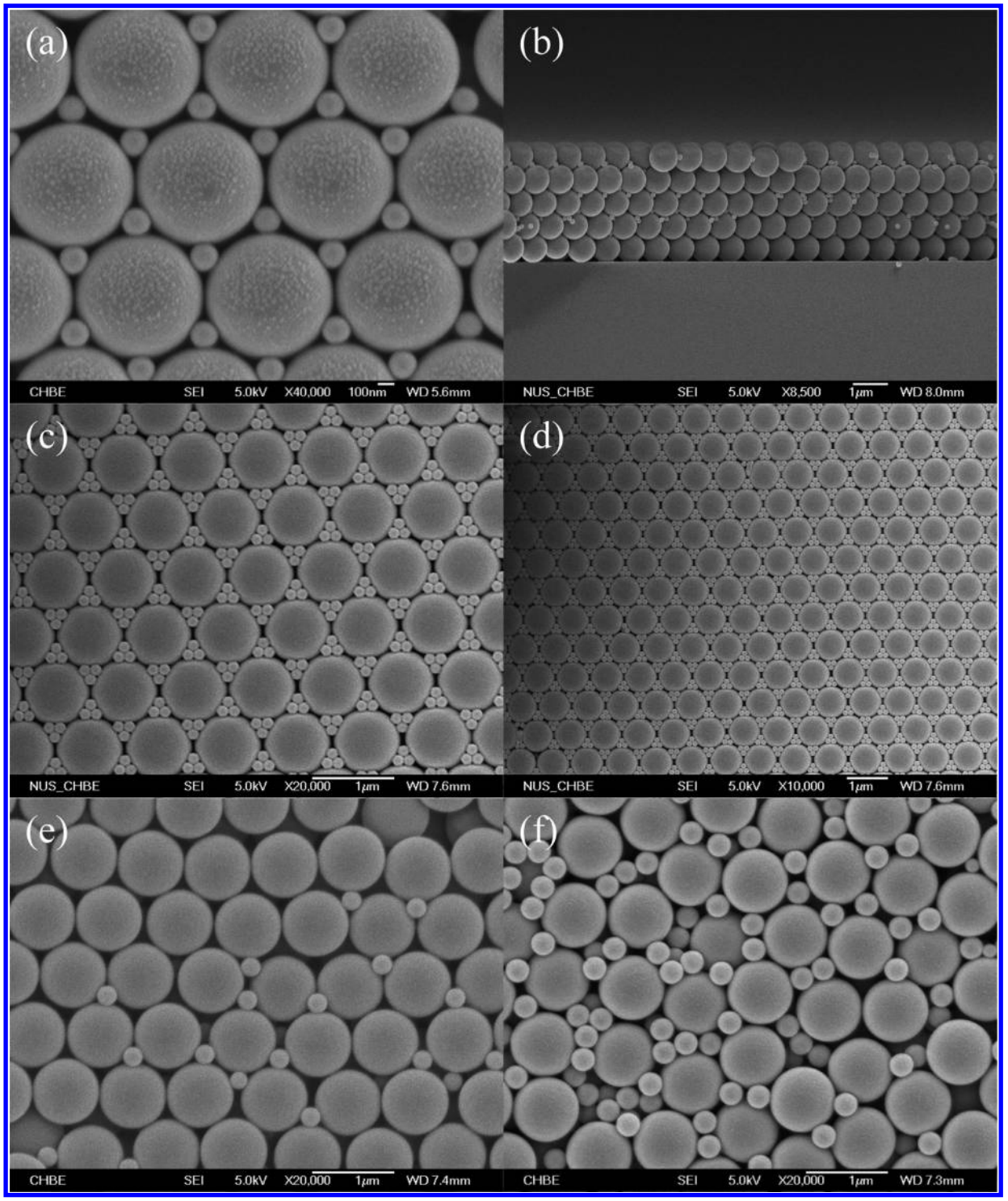

Figure 1. PS BCCs fabricated by conventional convective self-assembly method (without adding TEOS sol). (a) top view, 168/789 nm at $N_{S/L}$ = 2; (b) cross-sectional view, 168/789 nm at $N_{S/L}$ = 2; (c) high-magnification top view, 168/789 nm at $N_{S/L}$= 4; (d) low-magnification top view, 168/789 nm at $N_{S/L}$ = 4; (e) top views of BCCs, 227/789 nm at $N_{S/L}$ = 2; (f) top views of BCCs, 297/789 nm at $N_{S/L}$ = 2.

self-assembled structures of PS BCCs by increasing the size of small PS colloidal spheres from 168 to 297 nm while fixing the size of large PS colloidal spheres using the conventional self-assembly method. It was found that besides 168 nm colloidal spheres (Figure 1a–d), 178 nm ($\gamma_{S/L}$ = 0.225) PS colloidal spheres can also be self-assembled into ordered structure by using the conventional self-assembly method (see Figure S1b in the Supporting Information). Further increase in the size of small colloidal spheres size leads to less ordered BCCs (Figure 1e, f and Figure S2 in the Supporting Information). Figure 1e demonstrates a less ordered BCC fabricated with 227 and 789 nm colloidal spheres ($\gamma_{S/L}$ = 0.288). The large colloidal spheres remain much more ordered structure than that of small colloidal spheres. Figure 1f shows a typical SEM image of BCCs (297/789 nm) fabricated through conventional convective self-assembly method. As can be seen, there is almost no ordered

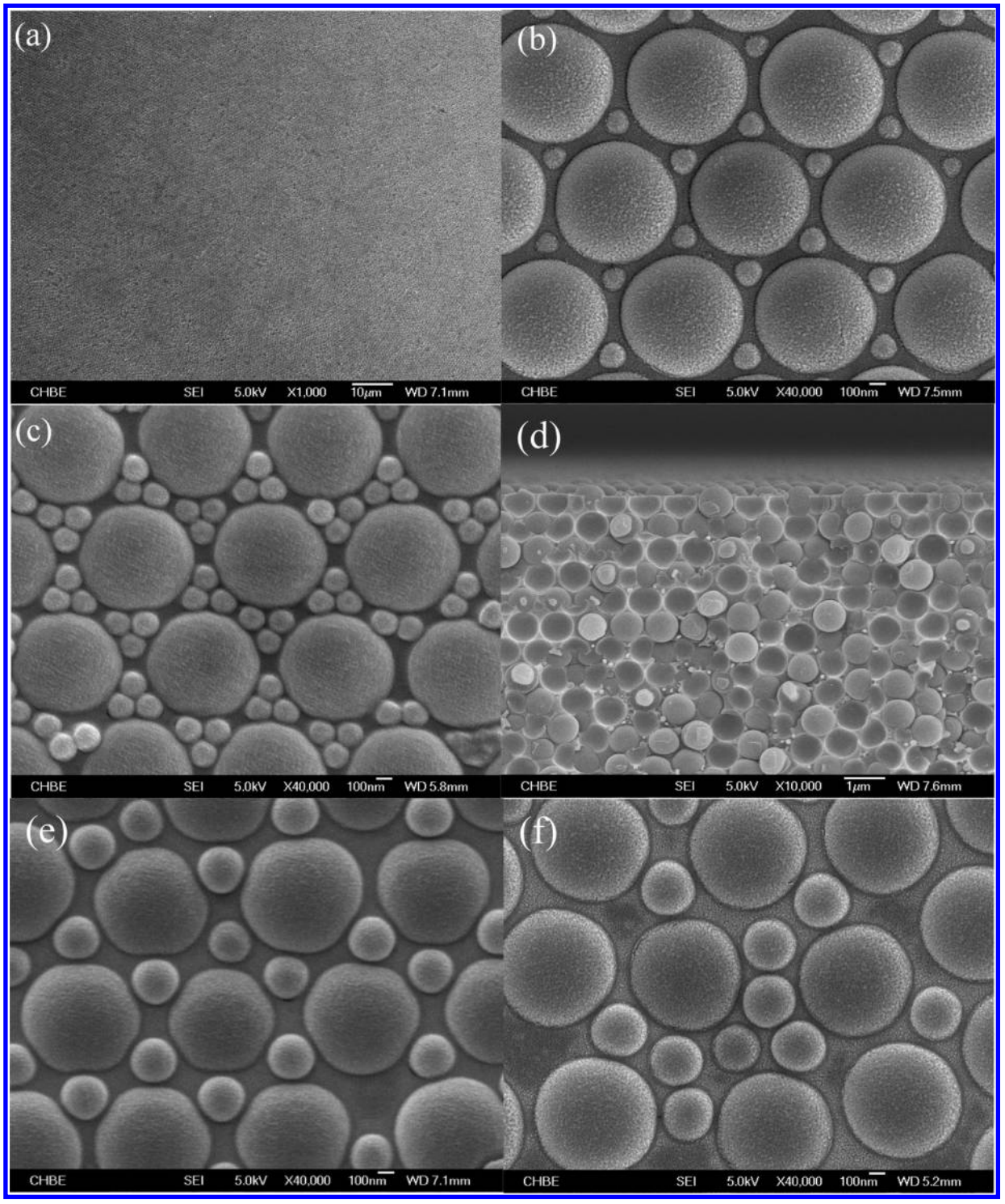

Figure 2. (a, b) Top views of 168/789 nm PS/SiO_2 BCCs at $N_{S/L}$ = 2; (c, d) top and cross-sectional views of 168/789 nm PS/SiO_2 BCCs at $N_{S/L}$ = 4; (e) 297/789 nm PS/SiO_2 BCCs at $N_{S/L}$ = 2; (f) 346/789 nm PS/SiO_2 BCCs at $N_{S/L}$ = 2.

structure for the colloidal sphere mixture with the size ratio of 0.376 (sphere size: 297 and 789 nm) using conventional self-assembly method. Some of the large spheres were surrounded by small spheres in a random way. Therefore, our experimental studies confirm that well-ordered BCCs cannot be formed using conventional convective self-assembly method when the size ratio is larger than 0.225. This is because in a close-packed fcc structure-based BCC, 0.225 is the largest relative size ratio that can be accommodated by a tetrahedral site.[9,22]

3.2. PS/SiO_2 BCCs (168/789, 297/789, and 346/789 nm) Fabricated by Improved Convective Self-Assembly Method. Figure 2 shows the SEM images of PS/SiO_2 BCCs fabricated at $N_{S/L}$ = 2 and $N_{S/L}$ = 4 using the improved self-assembly method. Figure 2a shows that BCCs can be fabricated in a large domain without cracks by using this improved convective self-assembly method (~100 × 100 μm^2). It is obvious that only one small sphere is embedded into each void among three large spheres in the horizontal plane (Figure 2b

and Figure S3a in the Supporting Information). Figure 2c demonstrates that there are three small spheres in the interstices formed by three large spheres in the same plane for $N_{S/L}$ = 4. A closer cross-sectional view of the samples also shows that the small PS colloidal spheres are embedded in the interstices of the large PS colloidal spheres (Figure 2d). Cross-sectional view of the PS/SiO_2 BCCs at low magnification confirms that the BCCs can be fabricated in relatively large area without cracks (see Figure S3b in the Supporting Information). This is consistent with our previous study that crack-free BCCs and their inverse structures were fabricated using a similar improved convective self-assembly method under optimized experimental conditions.[8] However, we did not recognize one important feature of this method in that study, that is, all the PS colloidal spheres (both small and large spheres) are not closely packed in PS/SiO_2 BCCs, whereas they are close-packed in PS BCCs fabricated with the conventional convective self-assembly method. The close-packed fcc configuration restricts the size ratios in BCCs. From this point of view, we postulate that this kind of BCCs could be fabricated with much extended size ratios.

As mentioned above, it was very challenging to obtain ordered binary structure when the size ratio is larger than 0.225 using the conventional convective self-assembly method. In contrast, for our improved self-assembly method by adding certain amount of freshly prepared TEOS sol, well-ordered structure with much extended size ratio is achieved with nonclose packed pattern. Figure S4 in the Supporting Information shows top views of PS/SiO_2 BCCs (227/789 nm) fabricated with the improved convective self-assembly method. As can be seen, well-ordered BCCs with extended size ratio were fabricated in relatively large area (200 μm × 200 μm). The inset fast Fourier transform (FFT) in Figure S4b in the Supporting Information indicates the long-range ordering of the resulting PS/SiO_2 BCCs. Figure 2e and Figure S5a in the Supporting Information show SEM images of PS/SiO_2 BCCs (297/789 nm) fabricated with the same method. We also fabricated BCCs with 346 and 485 nm PS as small spheres, which show less-ordered structure (Figure 2f and Figure S5b–d in the Supporting Information). The PS/SiO_2 BCCs fabricated with 346/789 nm show short-range ordering in the form of fcc (Figure 2f and Figure S5b in the Supporting Information). One can barely observe short-range ordering for the fabricated PS/SiO_2 BCCs with 485/789 nm using the improved convective self-assembly method, as shown in Figure S4c, d in the Supporting Information. These results indicate that our improved convective self-assembly method can extend the size ratio to 0.376 for well-ordered BCCs. The tunable size ratio range ($0.155 < \gamma_{S/L} < 0.376$) is broader than that in LbL techniques reported by Velikov and co-workers ($0.48 < \gamma_{S/L} < 0.54$).[14] The extended size ratios of the PS/SiO_2 BCCs probably can be attributed to the nonclose packed crystalline structure obtained from this method. The hydrolyzed TEOS sol forms interconnected networks and consequently results in a thin layer of silicate species between PS colloidal spheres as a result of polycondensation.

3.3. Optical Properties of the BCCs. Figure 3 shows the reflectance spectra of PS BCCs fabricated using 789 and 168 nm PS colloidal spheres at different number ratios. Distinct reflection peaks are clearly observed from the reflection spectra, indicating a well-ordered structure formed inside the BCCs. As the number ratio increases, the reflection peak intensity decreases, whereas the reflection peak position has a slight

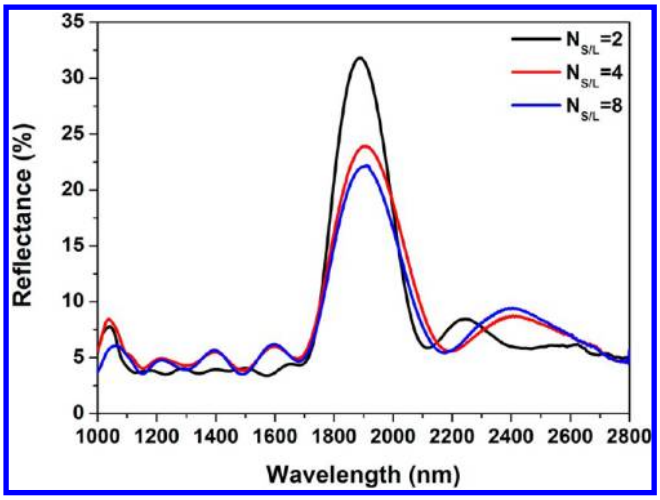

Figure 3. Reflection spectra of PS BCCs fabricated from 789 nm PS with 168 nm PS colloidal spheres at different number ratios.

redshift. The slight redshift of reflection peaks at higher number ratios is due to the increase in the effective refractive index caused by the high filling ratio of small PS colloidal spheres in the interstitial spaces of large PS colloidal spheres. The pronounced ripples on the reflection peaks of the BCCs can be treated as Fabry-Pérot fringes, which suggest that the refractive index varies among the crystal layers.[38]

To qualitatively compare both conventional and improved convective self-assembly methods, controlled experiments were further carried out to compare the optical properties of BCCs that consisted of the same large and small PS spheres. Figure 4 shows the optical spectra of BCCs fabricated from 789 nm PS with 168, 227, and 297 nm PS colloidal spheres, respectively, using these two self-assembly methods at $N_{S/L}$ = 2. Comparing the optical spectra of BCCs fabricated from both conventional (Figure 4a) and improved (Figure 4b) methods, several differences are observed: (1) The reflection peaks (i.e., the stop band positions) locate at different wavelengths, which is caused by the different lattices and effective refractive indices due to the addition of TEOS sol. (2) The PS/SiO_2 BCCs have a lower reflectance than BCCs fabricated from the conventional convective self-assembly method, which is attributed to the decreased effective refractive index contrast because of the infiltration of silicate species in the interstices of PS colloidal spheres;[39] it is noteworthy that the reflectance can be improved through increasing the thickness of the PS/SiO_2 BCCs film (see Figure S6 in the Supporting Information). (3) The PS/SiO_2 BCCs have a broader reflectance than the PS BCCs. We can see that at the fixed large sphere size, when the small sphere size increases, the reflection peak becomes broader for the BCCs fabricated from the improved convective self-assembly method. We speculate that the small spheres in the PS/SiO_2 BCCs cause much more scattering compared to the counterpart in the PS BCCs because the small spheres in the PS/SiO_2 BCCs are nonclose packed, which will have a bigger scattering cross-section compared to the close-packed case. This enhanced scattering will therefore result in the broadening of the reflection peak. (4) A closer look shows that a redshift is clearly observed from Figure 4a as the size ratio ($\gamma_{S/L}$) of the BCCs increases, which is similar to the observation in previous studies,[4,9] whereas no clear redshift is observed in Figure 4b. (5) As the size ratio ($\gamma_{S/L}$) of the BCCs increases, the reflectance decreases dramatically in Figure 4a. Especially, the

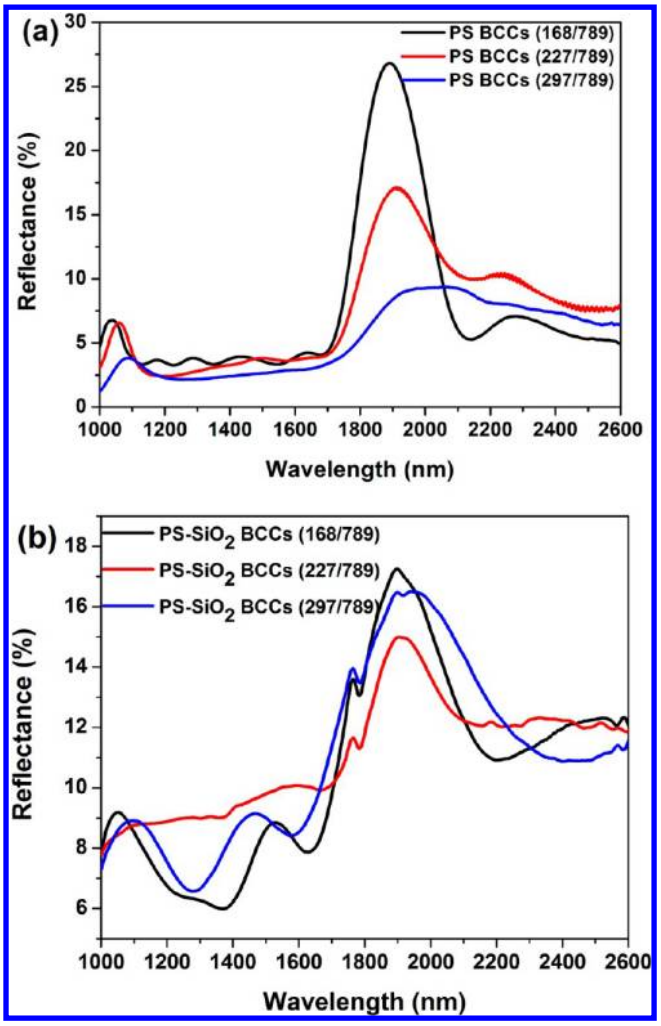

Figure 4. Reflection spectra of BCCs fabricated from 789 nm PS with 168, 227, and 297 nm PS colloidal spheres through (a) conventional and (b) improved convective self-assembly methods, respectively.

297/789 BCC has a reflectance less than 10% and a relatively broad peak, indicating that well-ordered structure is hard to achieve using conventional method when the size ratio is above a certain value. In contrast, definitive reflection peaks are still clearly observed for BCCs fabricated from the improved convective self-assembly method from Figure 4b, confirming well-ordered structures inside BCCs.

The reflection peak position of the BCCs can also be predicted by Bragg's equation: $\lambda_{max} = (8/3)^{1/2} D(n_{eff}^2 - \sin^2 \theta)^{1/2}$,[41,42] where λ_{max} is the wavelength of reflectance maxima, D is the diameter of large PS colloidal spheres, n_{eff} is the effective refractive index, and θ is the angle between the incident and the reflective surface along (111) plane. Here the refractive index of air is 1, and the refractive index of PS is 1.59, thus $n_{eff} = 1.4597$ (Here we assume that the fcc structure composing 74% spheres and 26% of the voids). For the PS/SiO_2 BCCs, the refractive index of SiO_2 is 1.45, thus $n_{eff} = 1.5548$ (Here we assume that the fcc structure composing 74% spheres and 26% of SiO_2 in the voids). The summarized experimental and calculated reflectance maxima are shown in Table 1. As can be seen, the experimental and calculated results are in good agreement except those BCCs fabricated from relatively large size ratios. Those PS/SiO_2 BCCs showed 100 nm differences between experimental and calculated values. However, the composition

Table 1. Calculated and Measured Stop Band Wavelengths

sample	assumed VF of large sphere in sample	assumed VF of small sphere in sample	calcd peak wavelength (nm)	measured peak wavelength (nm)
PS BCCs (2)	0.74	0.0143	1885	1886
PS BCCs (4)	0.74	0.0286	1900	1904
PS BCCs (8)	0.74	0.0572	1910	1912
PS BCCs (2)-168	0.74	0.0143	1885	1888
PS BCCs (2)-227	0.74	0.0352	1904	1910
PS BCCs (2)-297	0.74	0.0640	1923	2012
PS/SiO_2 BCCs (2)-168	0.74	0.0143	2006 (1906)[a]	1902
PS/SiO_2 BCCs (2)-227	0.74	0.0352	2009 (1918)[a]	1910
PS/SiO_2 BCCs (2)-297	0.74	0.0640	2015 (1936)[a]	1920

[a]The corrected values are 1906, 1918, and 1936 nm, respectively by using $n_{silicate} = 1.07$.[40]

in the voids of the BCCs is not real SiO_2 but hydrolyzed TEOS (also known as silicate species). The reported refractive index of silicate is as low as 1.07.[40] We corrected our assumption using the refractive index ($n = 1.07$) and got very good agreement with the measured results.

It should be noted that both the conventional and the improved convective self-assembly method can be used for the fabrication of PS/SiO_2 BCCs and PS BCCs. However, additional deposition of SiO_2 (for PS/SiO_2 BCCs) or removal of SiO_2 (for PS BCCs) step is necessary but unfavorable. Therefore, PS/SiO_2 BCCs and PS BCCs were chosen for the comparison. Comparing to conventional convective self-assembly method, PS/SiO_2 BCCs fabricated with improved convective self-assembly method have several distinct features: (1) PS colloidal spheres in PS BCCs are close-packed while they are nonclose packed in PS/SiO_2 BCCs. There is one thin layer of silicate species between two neighboring PS colloidal spheres in the same plane; (2) the extended size ratio can be achieved in PS/SiO_2 BCCs, whereas it is restricted in PS BCCs fabricated through the conventional convective self-assembly; (3) the PS BCCs fabricated with conventional convective self-assembly are 3D photonic crystals with void interstices, while the interstices of the PS/SiO_2 BCCs are filled with silicate species. Therefore, the average refractive index contrast of PS/SiO_2 BCCs is slightly larger than that of PS BCCs; (4) PS/SiO_2 BCCs fabricated in this method showed broadband reflectance comparing to PS BCCs.

3.4. Mechanism. Though the current improved convective self-assembly method is powerful in the fabrication of both well-ordered BCCs with much extended size ratios and crack-free BCCs, the mechanism has not been revealed. Comparing to BCCs fabricated with the conventional convective method, well-ordered BCCs can be fabricated with much extended size ratios by using the improved convective method. Obviously, the addition of TEOS sol into the colloidal suspension is the distinct feature of the improved convective self-assembly method. During the self-assembly process, TEOS sol plays a

pivotal role in the formation of PS/SiO_2 BCCs. First, the addition of TEOS sol enables the colloidal suspension into well-ordered colloidal arrays as the water-soluble polymer does.[32] It is well-known that particulate mobility is the key factor to form highly ordered crystalline structure and the convective flow of colloidal particles to the drying edge of the meniscus is fast during self-assembly.[43] Therefore, some of the colloidal particles may have insufficient time to move to thermodynamically favorable lattice sites during self-assembly. The presence of TEOS sol in the colloidal suspension would slow down the evaporation of the aqueous as a result of the increase in the viscosity of the mixture and thus allowing the colloidal particles to have sufficient time to organize into the lowest energy configuration.

Second, the addition of TEOS sol forms nonclose packed crystalline structure. The addition of polymeric binders (e.g., water-soluble polymer) has long been recognized to fabricate high-quality CCs.[32,34,44,45] However, the nonclose packed property of the resulting CCs was not revealed until the work on the fabrication of crack-free CCs using SiO_2 colloidal suspension and TEOS sol.[33] In that study, Wang and co-workers demonstrated key feature of this method, that is, crack-free and nonclose packed CCs can be made by adding TEOS sol into the colloidal suspension. This nonclose packed property though only exists in the same crystal plane, is crucial for the self-assembly of BCCs with extended size ratios. The nonclose packed configuration makes the size ratios larger than that in close-packed configuration as a result of extended constriction pore size.[9,22] This nonclose packed property is caused by the addition of TEOS sol. When applying TEOS sol during self-assembly, TEOS itself dissolves well in ethanol, its hydrolyzed form is hydrophilic and is therefore found inside the water-rich emulsion droplets. The polycondensation of TEOS will result in a thin layer of silicates in the interstices of PS spheres and consequently a nonclose packed colloidal crystal.[46]

Third, during colloids self-assembly, the TEOS sol that undergoes polycondensation provides a "glue" to the assembling PS colloidal spheres. The interconnected silicates networks provide sites of the relaxation of capillary force generated during self-assembly and dry stage under the catalysis of HCl, and thus inhibit the formation of cracks in the PS/SiO_2 BCCs composite films.[46,47] The addition of TEOS sol altered the colloidal suspension chemistry led to an increase in the strength of the film.[48] Therefore, the resulting BCCs show fewer cracks than their counterparts fabricated with the conventional convective self-assembly method.

3.5. Chemical Sensing. In recent years, chemo/biosensing using photonic crystals has attracted intense interests.[49−51] By using its virtue of average refractive index (RI) change caused diffraction shift, chemicals with different RI can be detected by BCCs. Figure 5 shows the influence of the media of varying RI upon the reflectance spectra of the BCCs. As can be seen, the diffraction peak redshifted from 1930 to 1959 nm as increases RI from 1.333 (water) to 1.399 (n-butanol), which can be attributed to the variation in the effective RI of the BCCs film. After calcination, one can obtained inverted structure of PS/SiO_2 BCCs, which may also find applications in sensing in addition to separation.[21] Thus, the resulting BCCs with tunable size ratios provide a better platform for engineering photonic bandgap structure and developing a broad range of applications such as photonics, spintronics, sensing, and bioseparation.

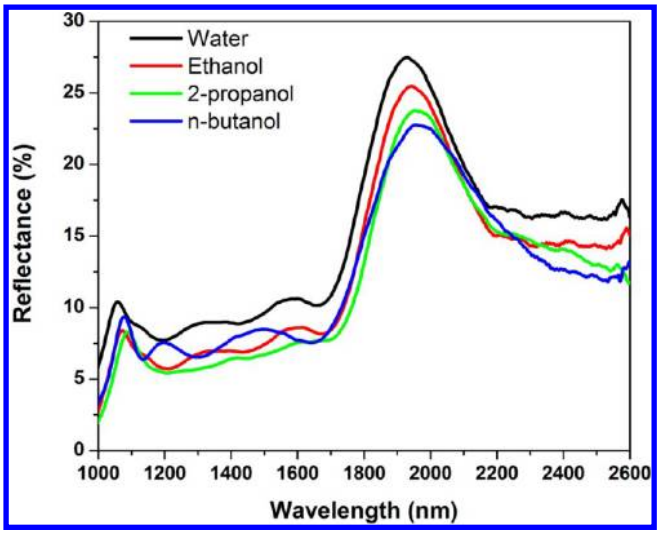

Figure 5. Reflectance spectra of the PS/SiO_2 BCCs (168/789) film in media of varying RI. The media used to fill the pores are water (n = 1.333), ethanol (n = 1.360), 2-propanol (n = 1.377), and n-butanol (n = 1.399).

4. CONCLUSIONS

A facile improved convective self-assembly method was presented and compared with the conventional method. It is found that the size ratios of the small to large PS for ordered BCCs can be extended to 0.376 because of the addition of the TEOS sol. Well-ordered nonclose packed PS/SiO_2 BCCs with size ratios of 0.213, 0.288, and 0.376, respectively, were fabricated and showed clear reflection peaks in the optical spectrum characterization. The new method enables the fabrication of BCCs with much extended size ratios and well-ordered crystalline structure. The extended size ratios give us much more freedom to engineer the photonic bandgap structures of BCCs and hence provide a better platform for developing various applications.

■ ASSOCIATED CONTENT

Supporting Information

The top view FESEM images of BCCs fabricated from 789, 168, 227, and 297 nm PS colloidal spheres; FESEM images of PS/SiO_2 BCCs fabricated from 789, 168, 227, 297, 346, and 485 nm PS colloidal spheres, and reflectance of the resulting PS/SiO_2 BCCs with larger thickness. This material is available free of charge via the Internet at http://pubs.acs.org/.

■ AUTHOR INFORMATION

Corresponding Authors

*E-mail: chemczy@gmail.com.

*E-mail: jh-teng@imre.a-star.edu.sg Telephone: +65-6874-8137. Fax: +65-6872-0785.

Notes

The authors declare no competing financial interest.

■ ACKNOWLEDGMENTS

Z.C. acknowledges a research scholarship from National University of Singapore. This work was supported by Agency for Science, Technology and Research (A*STAR) under Grant 0921540099 and 0921540098.

REFERENCES

(1) Bartlett, P.; Ottewill, R. H.; Pusey, P. N. Superlattice Formation in Binary Mixtures of Hard-Sphere Colloids. *Phys. Rev. Lett.* **1992**, *68*, 3801−3804.

(2) Yu, J.; Yan, Q.; Shen, D. Co-Self-Assembly of Binary Colloidal Crystals at the Air−Water Interface. *ACS Appl. Mater. Interfaces* **2010**, *2*, 1922−1926.

(3) Khalil, K. S.; Sagastegui, A.; Li, Y.; Tahir, M. A.; Socolar, J. E. S.; Wiley, B. J.; Yellen, B. B. Binary Colloidal Structures Assembled through Ising Interactions. *Nat. Commun.* **2012**, *3*, 794.

(4) Cai, Z.; Teng, J.; Xiong, Z.; Li, Y.; Li, Q.; Lu, X.; Zhao, X. S. Fabrication of TiO_2 Binary Inverse Opals without Overlayers via the Sandwich-Vacuum Infiltration of Precursor. *Langmuir* **2011**, *27*, 5157−5164.

(5) Vogel, N.; de Viguerie, L.; Jonas, U.; Weiss, C. K.; Landfester, K. Wafer-Scale Fabrication of Ordered Binary Colloidal Monolayers with Adjustable Stoichiometries. *Adv. Funct. Mater.* **2011**, *21*, 3064−3073.

(6) Kim, J. J.; Li, Y.; Lee, E. J.; Cho, S. O. Fabrication of Size-Controllable Hexagonal Non-Close-Packed Colloidal Crystals and Binary Colloidal Crystals by Pyrolysis Combined with Plasma−Electron Coirradiation of Polystyrene Colloidal Monolayer. *Langmuir* **2011**, *27*, 2334−2339.

(7) Zheng, Z.; Gao, K.; Luo, Y.; Li, D.; Meng, Q.; Wang, Y.; Zhang, D. Rapidly Infrared-Assisted Cooperatively Self-Assembled Highly Ordered Multiscale Porous Materials. *J. Am. Chem. Soc.* **2008**, *130*, 9785−9789.

(8) Cai, Z.; Teng, J.; Wan, Y.; Zhao, X. S. An Improved Convective Self-Assembly Method for the Fabrication of Binary Colloidal Crystals and Inverse Structures. *J. Colloid Interface Sci.* **2012**, *380*, 42−50.

(9) Wang, L.; Wan, Y.; Li, Y.; Cai, Z.; Li, H.-L.; Zhao, X. S.; Li, Q. Binary Colloidal Crystals Fabricated with a Horizontal Deposition Method. *Langmuir* **2009**, *25*, 6753−6759.

(10) Kitaev, V.; Ozin, G. A. Self-Assembled Surface Patterns of Binary Colloidal Crystals. *Adv. Mater.* **2003**, *15*, 75−78.

(11) Huang, X.; Zhou, J.; Fu, M.; Li, B.; Wang, Y.; Zhao, Q.; Yang, Z.; Xie, Q.; Li, L. Binary Colloidal Crystals with a Wide Range of Size Ratios via Template-Assisted Electric-Field-Induced Assembly. *Langmuir* **2007**, *23*, 8695−8698.

(12) Vermolen, E. C. M.; Kuijk, A.; Filion, L. C.; Hermes, M.; Thijssen, J. H. J.; Dijkstra, M.; van Blaaderen, A. Fabrication of Large Binary Colloidal Crystals with a NaCl Structure. *Proc. Natl. Acad. Sci. U.S.A.* **2009**, *106*, 16063−16067.

(13) Wan, Y.; Cai, Z.; Xia, L.; Wang, L.; Li, Y.; Li, Q.; Zhao, X. S. Simulation and Fabrication of Binary Colloidal Photonic Crystals and Their Inverse Structures. *Mater. Lett.* **2009**, *63*, 2078−2081.

(14) Velikov, K. P.; Christova, C. G.; Dullens, R. P. A.; van Blaaderen, A. Layer-by-Layer Growth of Binary Colloidal Crystals. *Science* **2002**, *296*, 106−109.

(15) Cai, Z.; Liu, Y. J.; Teng, J.; Lu, X. Fabrication of Large Domain Crack-Free Colloidal Crystal Heterostructures with Superposition Bandgaps Using Hydrophobic Polystyrene Spheres. *ACS Appl. Mater. Interfaces* **2012**, *4*, 5562−5569.

(16) Cong, H.; Cao, W. Array Patterns of Binary Colloidal Crystals. *J. Phys. Chem. B* **2005**, *109*, 1695−1698.

(17) Malekpourkoupaei, A.; Kostiuk, L. W.; Harrison, D. J. Fabrication of Binary Opal Lattices in Microfluidic Devices. *Chem. Mater.* **2013**, *25*, 3808−3815.

(18) Choi, H. K.; Im, S. H.; Park, O. O. Fabrication of Unconventional Colloidal Self-Assembled Structures. *Langmuir* **2010**, *26*, 12500−12504.

(19) Rengarajan, R.; Jiang, P.; Larrabee, D. C.; Colvin, V. L.; Mittleman, D. M. Colloidal Photonic Superlattices. *Phys. Rev. B* **2001**, *64*, 205103.

(20) Singh, G.; Gohri, V.; Pillai, S.; Arpanaei, A.; Foss, M.; Kingshott, P. Large-Area Protein Patterns Generated by Ordered Binary Colloidal Assemblies as Templates. *ACS Nano* **2011**, *5*, 3542−3551.

(21) Nazemifard, N.; Wang, L.; Ye, W.; Bhattacharjee, S.; Masliyah, J. H.; Harrison, D. J. A Systematic Evaluation of the Role of Crystalline Order in Nanoporous Materials on DNA Separation. *Lab Chip* **2012**, *12*, 146−152.

(22) Wang, J.; Ahl, S.; Li, Q.; Kreiter, M.; Neumann, T.; Burkert, K.; Knoll, W.; Jonas, U. Structural and Optical Characterization of 3D Binary Colloidal Crystal and Inverse Opal Films Prepared by Direct Co-Deposition. *J. Mater. Chem.* **2008**, *18*, 981−988.

(23) Singh, G.; Pillai, S.; Arpanaei, A.; Kingshott, P. Layer-by-Layer Growth of Multicomponent Colloidal Crystals Over Large Areas. *Adv. Funct. Mater.* **2011**, *21*, 2556−2563.

(24) Tan, K. W.; Li, G.; Koh, Y. K.; Yan, Q.; Wong, C. C. Layer-by-Layer Growth of Attractive Binary Colloidal Particles. *Langmuir* **2008**, *24*, 9273−9278.

(25) Wang, D.; Mohwald, H. Template-Directed Colloidal Self-Assembly - the Route to 'Top-Down' Nanochemical Engineering. *J. Mater. Chem.* **2004**, *14*, 459−468.

(26) Wang, D.; Möhwald, H. Rapid Fabrication of Binary Colloidal Crystals by Stepwise Spin-Coating. *Adv. Mater.* **2004**, *16*, 244−247.

(27) Kim, M. H.; Im, S. H.; Park, O. O. Fabrication and Structural Analysis of Binary Colloidal Crystals with Two-Dimensional Superlattices. *Adv. Mater.* **2005**, *17*, 2501−2505.

(28) Massé, P.; Ravaine, S. Engineered Multilayer Colloidal Crystals with Tunable Optical Properties. *Chem. Mater.* **2005**, *17*, 4244−4249.

(29) Zhou, Z.; Yan, Q.; Li, Q.; Zhao, X. S. Fabrication of Binary Colloidal Crystals and Non-Close-Packed Structures by a Sequential Self-Assembly Method. *Langmuir* **2006**, *23*, 1473−1477.

(30) Hatton, B.; Mishchenko, L.; Davis, S.; Sandhage, K. H.; Aizenberg, J. Assembly of Large-Area, Highly Ordered, Crack-Free Inverse Opal Films. *Proc. Natl. Acad. Sci. U S A* **2010**, *107*, 10354−10359.

(31) Cai, Z.; Liu, Y. J.; Leong, E. S. P.; Teng, J.; Lu, X. Highly Ordered and Gap Controllable Two-Dimensional Non-Close-Packed Colloidal Crystals and Plasmonic-Photonic Crystals with Enhanced Optical Transmission. *J. Mater. Chem.* **2012**, *22*, 24668−24675.

(32) Kim, M. H.; Choi, H. K.; Park, O. O.; Im, S. H. Fabrication of Robust, High-Quality Two-Dimensional Colloidal Crystals from Aqueous Suspensions Containing Water-Soluble Polymer. *Appl. Phys. Lett.* **2006**, *88*, 143127−3.

(33) Wang, L.; Zhao, X. S. Fabrication of Crack-Free Colloidal Crystals Using a Modified Vertical Deposition Method. *J. Phys. Chem. C* **2007**, *111*, 8538−8542.

(34) Zhou, J.; Wang, J.; Huang, Y.; Liu, G.; Wang, L.; Chen, S.; Li, X.; Wang, D.; Song, Y.; Jiang, L. Large-Area Crack-Free Single-Crystal Photonic Crystals via Combined Effects of Polymerization-Assisted Assembly and Flexible Substrate. *NPG Asia Mater.* **2012**, *4*, e21.

(35) Cai, Z.; Liu, Y. J.; Lu, X.; Teng, J. In Situ "Doping" Inverse Silica Opals with Size-Controllable Gold Nanoparticles for Refractive Index Sensing. *J. Phys. Chem. C* **2013**, *117*, 9440−9445.

(36) Singh, G.; Griesser, H. J.; Bremmell, K.; Kingshott, P. Highly Ordered Nanometer-Scale Chemical and Protein Patterns by Binary Colloidal Crystal Lithography Combined with Plasma Polymerization. *Adv. Funct. Mater.* **2011**, *21*, 540−546.

(37) Shim, S. E.; Cha, Y. J.; Byun, J. M.; Choe, S. Size Control of Polystyrene Beads by Multistage Seeded Emulsion Polymerization. *J. Appl. Polym. Sci.* **1999**, *71*, 2259−2269.

(38) Reculusa, S.; Ravaine, S. Synthesis of Colloidal Crystals of Controllable Thickness through the Langmuir−Blodgett Technique. *Chem. Mater.* **2003**, *15*, 598−605.

(39) Liu, Y. J.; Cai, Z.; Leong, E. S. P.; Zhao, X. S.; Teng, J. H. Optically Switchable Photonic Crystals Based on Inverse Opals Partially Infiltrated by Photoresponsive Liquid Crystals. *J. Mater. Chem.* **2012**, *22*, 7609−7613.

(40) Yamaguchi, M.; Nakayama, H.; Yamada, K.; Imai, H. Ultralow Refractive Index Coatings Consisting of Mesoporous Silica Nanoparticles. *Opt. Lett.* **2009**, *34*, 2060−2062.

(41) Schroden, R. C.; Al-Daous, M.; Blanford, C. F.; Stein, A. Optical Properties of Inverse Opal Photonic Crystals. *Chem. Mater.* **2002**, *14*, 3305−3315.

(42) Cai, Z.; Teng, J.; Yan, Q.; Zhao, X. S. Solvent Effect on the Self-Assembly of Colloidal Microspheres via a Horizontal Deposition Method. *Colloid Surf., A* **2012**, *402*, 37−44.
(43) Tan, K. W.; Koh, Y. K.; Chiang, Y.-M.; Wong, C. C. Particulate Mobility in Vertical Deposition of Attractive Monolayer Colloidal Crystals. *Langmuir* **2010**, *26*, 7093−7100.
(44) Jiang, P.; McFarland, M. J. Large-Scale Fabrication of Wafer-Size Colloidal Crystals, Macroporous Polymers and Nanocomposites by Spin-Coating. *J. Am. Chem. Soc.* **2004**, *126*, 13778−13786.
(45) Cai, Z.; Xiong, Z.; Lu, X.; Teng, J. In Situ Gold-Loaded Titania Photonic Crystals with Enhanced Photocatalytic Activity. *J. Mater. Chem. A* **2014**, *2*, 545−553.
(46) Brinker, C. J.; Scherer, G. W. *Sol−Gel Science: The Physics and Chemistry of Sol−Gel Processing*; Academic Press: New York, 1990.
(47) Iler, R. K. *The Chemistry of Silica: Solubility, Polymerization, Colloid and Surface Properties and Biochemistry of Silica*; John Wiley & Sons: New York, 1979.
(48) Prosser, J. H.; Brugarolas, T.; Lee, S.; Nolte, A. J.; Lee, D. Avoiding Cracks in Nanoparticle Films. *Nano Lett.* **2012**, *12*, 5287−5291.
(49) Fenzl, C.; Hirsch, T.; Wolfbeis, O. S. Photonic Crystals for Chemical Sensing and Biosensing. *Angew. Chem., Int. Ed.* **2014**, *53*, 3318−3335.
(50) Cai, Z.; Zhang, J.-T.; Xue, F.; Hong, Z.; Punihaole, D.; Asher, S. A. 2D Photonic Crystal Protein Hydrogel Coulometer for Sensing Serum Albumin Ligand Binding. *Anal. Chem.* **2014**, *86*, 4840−4847.
(51) Ge, J.; Yin, Y. Responsive Photonic Crystals. *Angew. Chem., Int. Ed.* **2011**, *50*, 1492−1522.